GEOMETRIC AND RADIOMETRIC CORRECTION OF ESA SAR PRODUCTS

David Small[(1)], Adrian Schubert[(1)] , Betlem Rosich[(2)] , Erich Meier[(1)]

[(1)] Remote Sensing Laboratories (RSL), University of Zürich, Winterthurerstrasse 190, CH-8057 Zürich, Switzerland, Email: david.small@geo.uzh.ch

[(2)] ESA-ESRIN, Via Galileo Galilei - 00044 Frascati (ROME), Italy, Email: betlem.rosich@esa.int

ABSTRACT

Accurate geolocation of SAR imagery enables not only precise overlays with other data sources in a common map geometry, but also normalisation for the systematic influence of terrain on image radiometry. We begin by describing our verifications of the geometric behaviour of ENVISAT ASAR products, including all image mode (IM), alternating polarisation (AP), and wide swath (WS) types: IMS, IMP, IMM, IMG, APS, APP, APM, APG, WSM, and WSS. Radar transponders in Canada and Europe are used as easily identifiable targets in radar images to test the accuracy of the nominal timing and state vector annotations accompanying each product. Accuracies achievable using DORIS precise state vectors are also evaluated. In addition to ENVISAT's ASAR, geolocation accuracies achievable using ERS-1/2 and ALOS PALSAR data are demonstrated. Given accurate knowledge of the acquisition geometry of a SAR image from one of the above sensors together with a digital elevation model (DEM) of the area imaged, the process of *terrain geocoding* is used to transform a diverse set of images into a common reference map geometry. The prerequisite DEM combined with accurate knowledge of the acquisition geometry also enables a *radiometric correction*, whereby variations in terrain specific to each scene are normalised to a common standard. Thematic interpretation benefits from such pre-processing: we demonstrate improved thematic discriminations using product overlays in a common map geometry where *radiometric terrain correction* (RTC) has been applied in comparison to typical GTC results.

1 INTRODUCTION

The wide variety of SAR imaging sensors, modes, and product types provides a striking diversity of capabilities. Every product received by a user was originally designed trading off parameters such as resolution against swath width, number of polarisations, file size, etc. Allowing seamless inter-comparison of SAR images from differing sensors, modes, and product types requires both rigorous geometric and radiometric calibration. We review relative and absolute geometric validation results for the ENVISAT ASAR modes: "IM" (Image Mode), "AP" (Alternating Polarisation), and "WS" (Wide Swath). For each mode, we compare the geometric characteristics of each product type: for IM, that is Single-Look-Complex (SLC) IMS, ground range precision (IMP), medium resolution (IMM), and full resolution geocoded ellipsoid corrected (IMG); likewise for the AP mode: slant range SLC APS, ground range precision (APP), medium resolution (APM), and the ellipsoid geocoded (APG). In the wide swath "WS" case, we consider the two product types: medium resolution (WSM) and wide swath SLC (WSS). After illustrating the *relative* consistency of the above range of product types, we illustrate also the *absolute* accuracy of their timing annotations in allowing highly accurate prediction of a given target's location in the image. In the case of data from other sensors such as ERS-2, the orbital state vectors are not as accurate as in the case of ENVISAT. In cases such as these, radar image simulation can be used generate a synthetic SAR image based on the best available DSM. Correlation between the real image and the synthetic one reveals differences in timing parameters (e.g. near range and azimuth start time) that can be used to improve the knowledge of the scene's geometry [8]. The same image simulation methodology also allows rigorous normalisation of the radar backscatter for the local illuminated area. In the absence of such knowledge, the conversion from β^0 to γ is performed assuming that the local incidence angle is determined by a nominal ellipsoid geometry [3]. We show that more detailed accounting for the local illuminated area allows improved retrieval of the radar backscatter coefficient.

2 GEOMETRIC CALIBRATION

Successful geolocation requires accurate knowledge of the acquisition geometry. The range and azimuth sample spacing are both generally well-known; in addition, one requires the near-range "sampling window start time" and the azimuth start time in the time annotation system chosen (e.g. Zero-Doppler or Doppler centroid), and in the case of ground range products, the slant/ground range polynomial coefficients.

2.1 ASAR

We tested both the *relative* accuracy of the relevant annotations (between different product types generated from the same image acquisition) and their *absolute* geolocation accuracy (using transponder targets with accurately surveyed locations). In the IM and AP product sets, the IMG and APG ellipsoid geocoded product types are the only ones not in a path orientation. To compare all four products in a common geometry, we therefore chose to first ellipsoid-geocode the other

Proc. 'Envisat Symposium 2007', Montreux, Switzerland
23–27 April 2007 (ESA SP-636, July 2007)

products into the same map geometry as the IMG or APG, and search for any systematic biases between the resulting "GEC" images. We compared IMS-GEC, IMP-GEC, IMM-GEC and IMG products directly in the IMG geometry. Figure 1 shows RGB overlays of three of the four IM or AP product types. The azimuth start and stop times varied between product types, with a large overlap zone. The small area in the red box is shown in greater detail below the overview image. In Figure 1(a), a very high consistency between the 3 product types is evident. The largest difference visible is (as expected) that the medium resolution IMM product inherently has a lower resolution. Most product sets investigated exhibited similar behaviour. In rare cases however, an intermittent range bias [6] was found to cause relative shifts. IMS, IMP, & IMG products can be subject to the shift while no IMM products have yet been observed to exhibit the shift. In such cases, an RGB overlay of an IMM-GEC with any other IM product in IMG geometry shows that the IMS/IMP/IMG products are shifted with respect to the IMM. Such a case is illustrated in Figure 1(b). A typical AP case is shown in Figure 1(c). No significant shift between the APG product and the APS-GEC & APP-GEC are apparent. However, rare cases have been observed where the APS product type is susceptible to the same intermittent range bias, but not the APP, APM or APG product types. In addition to these qualitative image overlays, we used image correlation [5] to retrieve quantitative estimates of inter-product geometric biases. Table 1 lists the means and standard deviations measured for IMG vs. IMS/IMP/IMM & APG vs. APS/APP/APM Netherlands products. Note that the IMM/APM products have a sample spacing of 75m. Inter-product geometric consistency is within less than a third of a product sample size.

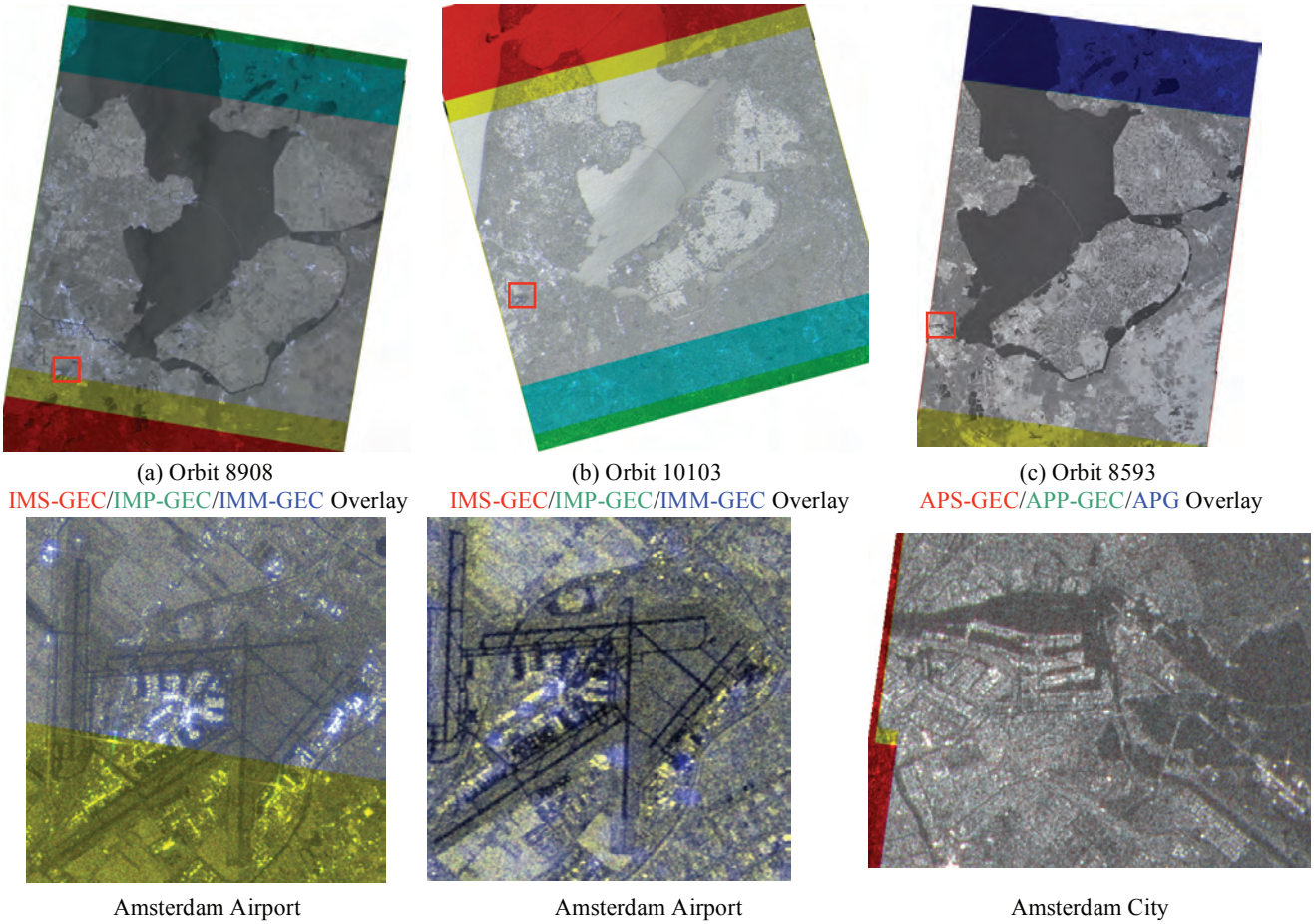

(a) Orbit 8908
IMS-GEC/IMP-GEC/IMM-GEC Overlay

(b) Orbit 10103
IMS-GEC/IMP-GEC/IMM-GEC Overlay

(c) Orbit 8593
APS-GEC/APP-GEC/APG Overlay

Amsterdam Airport

Amsterdam Airport

Amsterdam City

Figure 1. Netherlands RGB Overlays in IMG/APG product map geometries

Table 1. Relative Consistencies between ASAR IM/AP Product Types (rare intermittent range bias cases excepted)

IM	Easting [m]	Northing [m]	**AP**	Easting [m]	Northing [m]
IMS-GEC vs. IMG	-1.7±3.0	0.65±2.7	APS-GEC vs. APG	0.61±3.8	0.02±4.9
IMP-GEC vs. IMG	-1.6±1.5	0.59±0.59	APP-GEC vs. APG	0.80±2.3	0.27±3.2
IMM-GEC vs. IMG	-5.8±16	-0.06±16	APM-GEC vs. APG	-8.2±11	5.2±13

2.2 Absolute Geolocation Accuracy

In addition to the tests of *relative* accuracy described above, we also tested the *absolute* geolocation accuracy using data acquired over transponders. The transponder image location is *predicted* by solving the range and Doppler equations [7] and compared to an actual *measurement* of its strong response within the image. Differences between predicted and measured locations can be caused by inaccuracies in the radar timing annotations or orbital state vectors employed during geolocation. Figure 2 illustrates absolute geolocation accuracies for APS, APP, and APM products acquired over the Netherlands ASAR transponders. Note that the intermittent range bias described above is observed (rarely) in APS products, but never to date in APP, APM, or APG products [6]. The only product types observed to be affected by the rare bias are IMS, IMP, IMG, and APS. These product types all flow through a Range-Doppler input chain, whereas IMM, APP, APM, and APG products all use a different input chain developed for their SPECAN processor. The rare bias can cause a slant range shift of approximately twelve samples and is being further investigated.

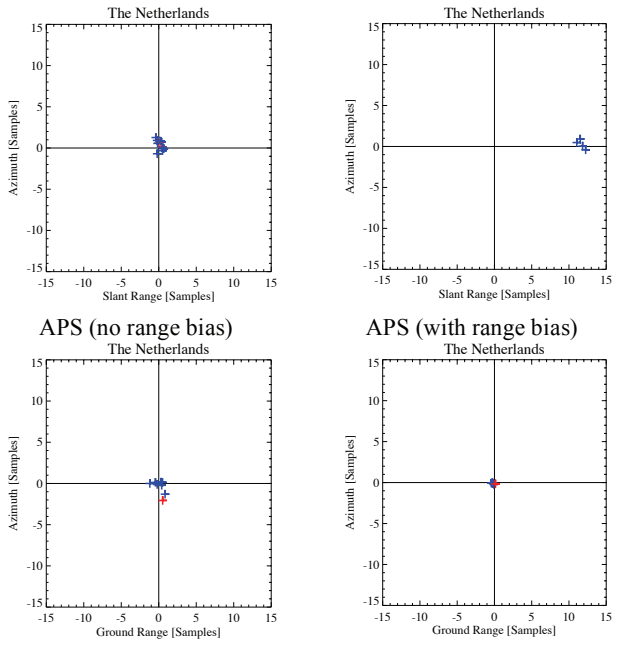

Figure 2. Netherlands ASAR Transponder AP product localisation: Predicted vs. Measured Positions

In addition to the standard geolocation accuracy tests performed using the DORIS precise state vector products, we compared those results with the geolocation accuracy achievable using predicted, restituted, and DORIS preliminary as well as the geolocation grid annotated in the product. These state vector qualities are available before the acquisition, or hours to days afterwards, and can be the only alternative for users processing ASAR data in a near-real-time (NRT) context. Figure 3 juxtaposes accuracy results using each of the four state vector product types for IM acquisitions over Resolute, Canada. Note that restituted, preliminary, and precise state vectors all achieve accuracy unprecedented in previous spaceborne SAR sensors, with the geolocation accuracy within a single high-resolution IMS sample. The predicted orbits understandably have a lower accuracy that decreases as the interval between the time of their generation (before the acquisition) and the acquisition time increases. A close-up comparison of the restituted and precise orbit accuracies is shown in Figure 4. Note that although the geolocation predictions based on restituted state vectors are slightly less accurate than those based on preliminary or precise orbits, they far exceed the accuracy of results from the generation of SAR sensors before ENVISAT.

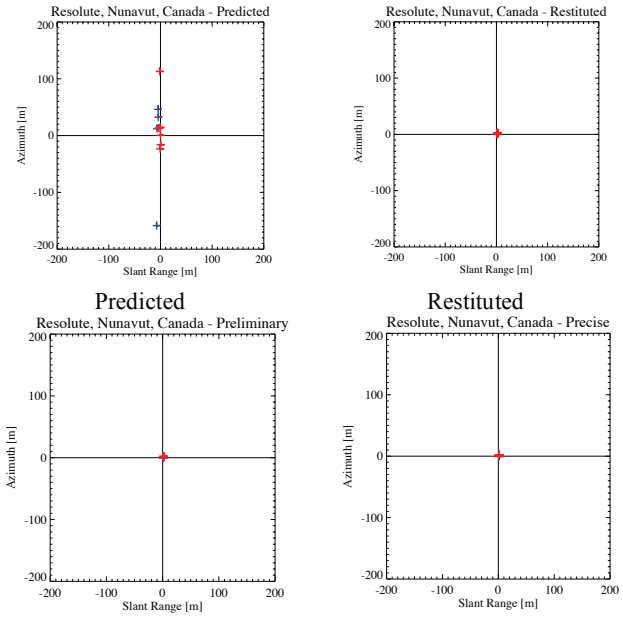

Figure 3. Resolute (Canada) RADARSAT Transponder ASAR IMS product localisation accuracy according to state vector product type (ascending/descending are colour coded)

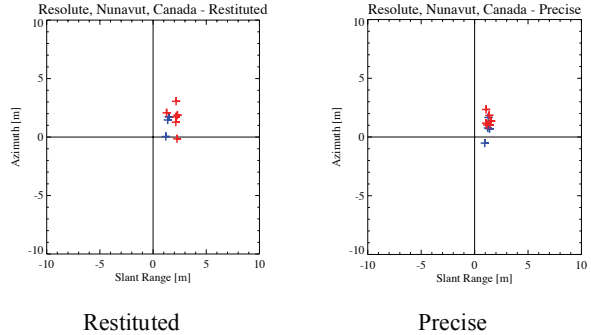

Figure 4. Resolute (Canada) RADARSAT Transponder ASAR IMS product localisation: Very high accuracy using restituted, preliminary or precise state vectors

2.3 Radar Image Simulation

Older sensors such as the ERS satellites were unfortunately unable to provide such high quality state vectors. For SAR sensors where the geometry is less well known, one can improve the parameterisation of the scene geometry by using the technique of radar image simulation to produce a synthetic radar amplitude image and using real to synthetic image-to-image correlation [5] to estimate local offsets between the two images. One can then summarise the offset field with a model of range and azimuth start time biases. Assuming a DEM of comparable resolution, that the initial state vectors are moderately accurate and that the initial image simulation is therefore highly correlated to the real image, the result provides improved knowledge of the range and azimuth timing parameters, which often suffice to enable accurate terrain geocoding [8]. Examples of actual and simulated ERS-2 amplitude images are shown in Figure 5(a). The two images are overlaid after co-registration in Figure 5(b). In addition to providing improved knowledge of geometry if necessary, image simulation also enables more rigorous derivation of radar backscatter γ and σ^0 from β^0 by normalising for the actual local illuminated area rather than the ellipsoid-model-based approximation still dominant in SAR image analysis

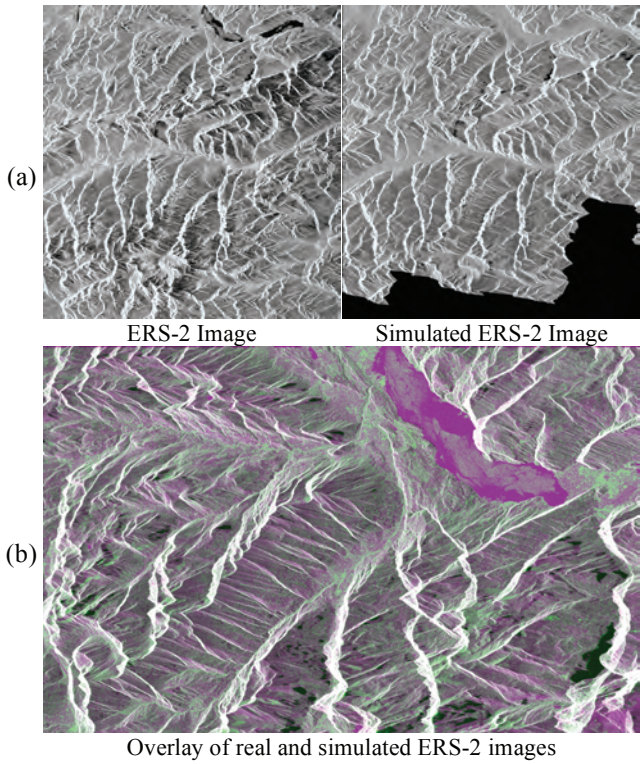

Figure 5. ERS-2 Real and Simulated Images of Interlaken, Switzerland – 2006.09.06

2.4 ALOS PALSAR

In the case of CEOS level 1.1 (SLC) PALSAR data processed using the JAXA processor, the data is not presented in Zero-Doppler annotation. Instead a polynomial with range-dependent Doppler coefficients is stored in the product that must be applied during geolocation. Two coefficients were stored in the products investigated, providing a model of "linear Doppler" variation. Since ALOS employs yaw steering, the variation is small and can be well modelled with two coefficients. We deployed corner reflectors outside of Zürich that were imaged by PALSAR in FBS and FBD modes. Predicted locations of the reflectors are compared to their actual positions in Figure 6. Note how all products exhibit a similar azimuth shift for this test site. All products were annotated with ALOS precise quality state vectors. Examples of geocoded PALSAR images are shown in Figure 7. Those in the top row are conventional geocoded terrain corrected "GTC" products while those below have had their backscatter normalised by the local illuminated area. Overlays of the images are shown in Figure 8.

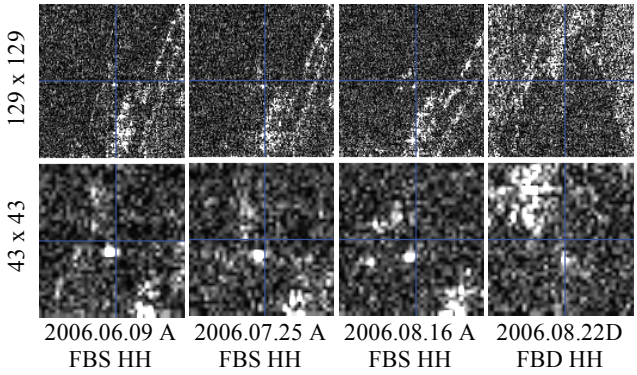

Figure 6. Zürich PALSAR Corner Reflector: Predicted (blue cross) vs. measured positions in SLC products

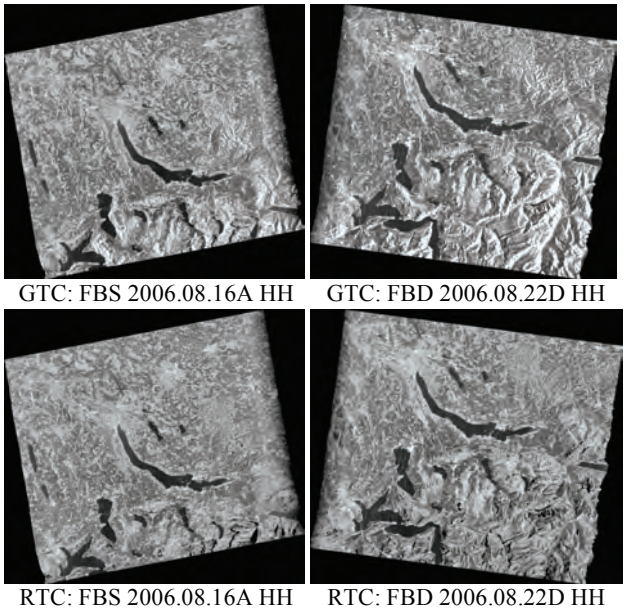

Figure 7. Comparison of Zürich PALSAR: FBS 2006.08.16A and FBD 2006.08.22D as GTC and RTC

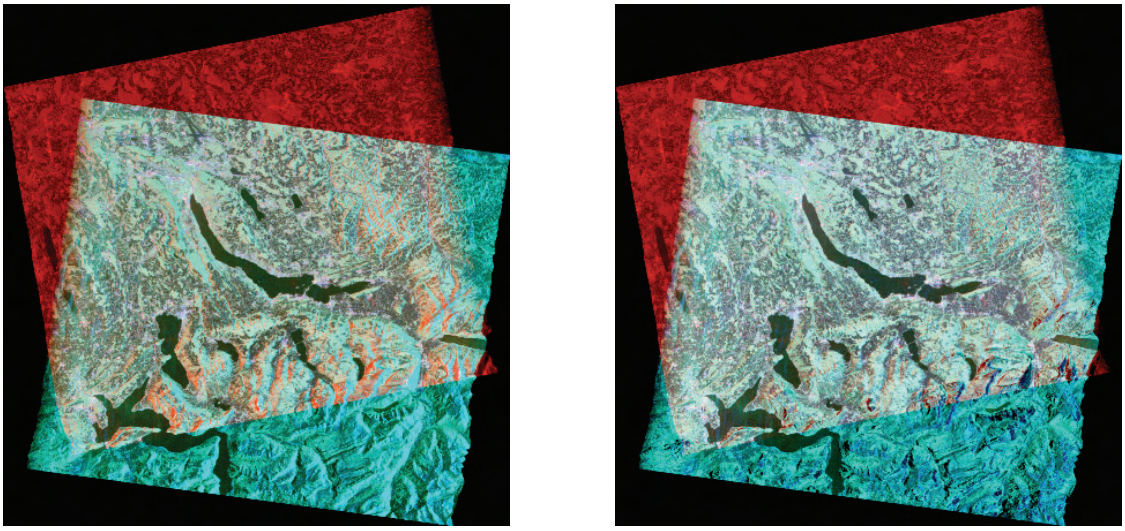

(a) Geocoded Terrain Corrected (GTC) (b) Radiometrically Terrain Corrected (RTC)

Figure 8. Overlay of Zürich PALSAR images: FBS 2006.08.16A (R=HH) and FBD 2006.08.22D (G=HV, B=HH) as (a) GTC and (b) RTC

Note how inter-comparison of information from ascending/descending passes is polluted by topographic influences in the GTC case; much less so in the RTC case.

2.5 ASAR WSM Terrain Correction

Terrain correction incorporating normalisation for local illuminated area has particularly large effects in scenes with large variations in nominal incidence angle such as ASAR Wide-Swath (WS) mode and significant topography. A comparison of conventional "GTC" terrain correction with radiometric terrain correction "RTC" is shown in Figure 9 and Figure 10 where three WS datasets were acquired from differing tracks. Note how the backscatter information is a mixture of terrain-induced and thematic effects in the GTC case. In the RTC case, thematic differences between the three images overlaid are much clearer. It appears that a melt event in the April 2006 (green channel) produced decreased backscatter in comparison to the two other dates (confirmed by meteo station records).

3 CONCLUSIONS

The increasing number of SAR image sources and modes continually increases the importance of high quality geometric localisation and radiometric calibration to enable meaningful inter-comparisons. The ASAR sensor provides unprecedented localisation accuracy across a diverse set of product types. Their relative and absolute geometric accuracies have been confirmed to be well within specification, usually achieving accuracies within a single sample (even in the high resolution SLC product types). Initial results confirm also a high PALSAR geometric accuracy. High local radiometric accuracy is best achieved by normalising for local illuminated area. It was demonstrated that interpretation of multi-track ASAR or PALSAR inter-comparisons benefit from such normalisations, resulting in improved retrieval of thematic information and geophysical variables.

4 ACKNOWLEDGMENTS

The ALOS PALSAR products were provided to RSL by ESA for RSL's subcontract to SARMAP's "PALSAR Verification Processor" Contract [2] No. 19566/06/I-OL. The ASAR geometric calibration work was supported by ESRIN contract 19668/06/I-EC. The reference DHM25 height model provided by the Swiss Federal Office of Topography was used for geometric and radiometric corrections. Thanks to Linda Valenti (RSL) for preparing and providing the meteorological information.

5 REFERENCES

1. ESA SPPA Manager, *ENVISAT ASAR AP Product Quality Disclaimer*, ENVI-GSOP-EOGD-QD-05-0082, http://envisat.esa.int/dataproducts/availability/disclaimers/PQD_0082ASA_all.pdf
2. Pasquali P., Guarnieri A.M., D'Aria D., et al., ALOS PALSAR Verification Processor, *Proc. ENVISAT Symposium*, Montreux, Switzerland, April 23-27, 2007.
3. Rosich B., Meadows P., Absolute Calibration of ASAR Level 1 Products Generated with PF-ASAR, *ENVI-CLVL-EOPG-TN-03-0010*, ESA-ESRIN, Frascati, Italy, 7 Oct 2004.
4. Schubert A., Small D., Rosich B., Meier E., ASAR WSS Product Verification using Derived Image Mosaics, *Proc. ENVISAT Symposium*, Montreux, Switzerland, April 23-27, 2007.
5. Schubert A., Small D., Meier E., Nüesch D., Extraction of Surface Topography from SAR Images Using Combined Interferometry and Stereogrammetry, *Proc. EUSAR 2004*, Ulm, Germany, May 25-27, 2004, pp. 775-778.
6. Small D., Rosich B., Schubert A., Meier E., ENVISAT ASAR Geometric Validation, *Proc. CEOS SAR Workshop*, Edinburgh, United Kingdom, Oct. 3-6, 2006 (in press).
7. Small D., Rosich B., Schubert A., Meier E., Nüesch D., Geometric Validation of Low and High-Resolution ASAR Imagery, *Proc. 2004 ENVISAT & ERS Symposium*, Salzburg, Austria, Sept. 6-10, 2004 (ESA SP-572, April 2005). 9p.
8. Small D., Biegger S., Nüesch D., Automated Tiepoint Retrieval through Heteromorphic Image Simulation for Spaceborne SAR Sensors, *Proc. 2000 ERS-ENVISAT Symposium*, Gothenburg, Sweden, Oct. 16-20, 2000 (ESA SP-461). 8p.

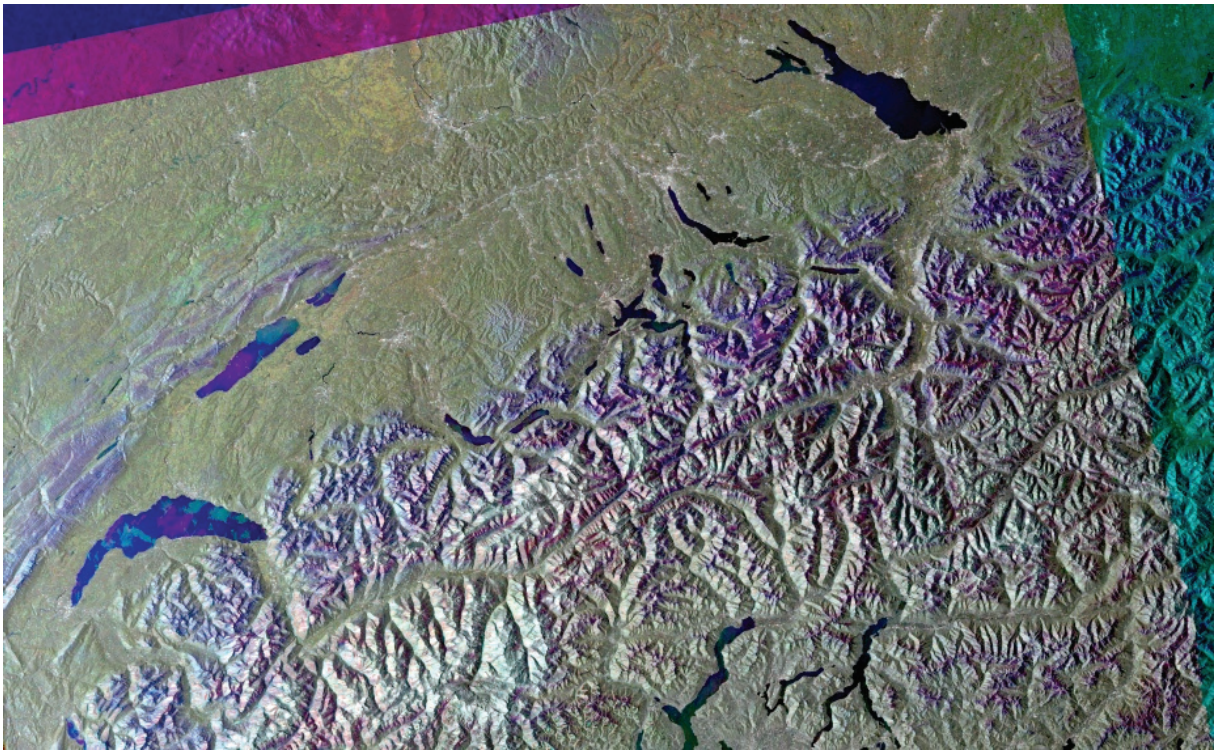

Figure 9. Switzerland: Geocoded Terrain Corrected (GTC) ASAR WSM VV Products: R=2007.03.03, G=2006.04.03, B=2006.01.23

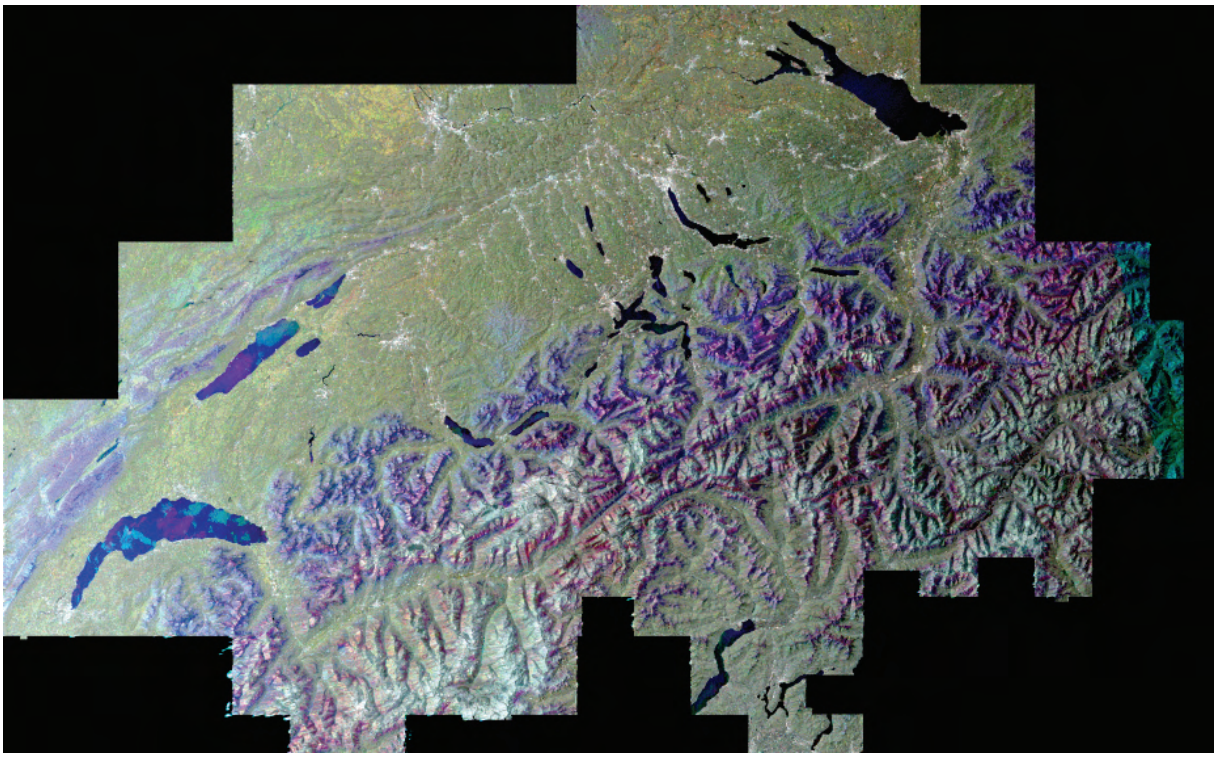

Figure 10. Switzerland: Radiometrically Terrain Corrected (RTC) ASAR WSM VV Products: R=2007.03.03, G=2006.04.03, B=2006.01.23; DHM25 courtesy Swiss Federal Office of Topography